Electronic Supporting Information

Efficient Electroosmotic Mixing in a Narrow-Fluidic Channel: The Role of a Patterned Soft Layer

Harshad Sanjay Gaikwad[1], Gaurav Kumar[2], Pranab Kumar Mondal*[1].

[1]Microfluidcs and Microscale Transport Processes Laboratory,
Department of Mechanical Engineering, Indian Institute of Technology Guwahati, Assam, India – 781039
[2]Department of Mechanical Engineering, Cochin University of Science and Technology, Kerala, India - 682022

Corresponding Author*:-mail2pranab@gmail.com; pranabm@iitg.ac.in

* Email: mail2pranab@gmail.com; pranabm@iitg.ac.in

S1. Weak-field approximation

In the present study, the magnitude of the external electric field (E_0) is of the order of $O\left[10^3\right]$ whereas the magnitude of the induced electric field is of the order of $O\left[10^6\right]$. To estimate the order of induced field, we consider that the induced electrostatic potential $\left(k_B T\right)/ze$ is of the order of 10^1 mV $\left(\zeta = |25|\text{mV}\right)$, and the Debye length is of the order of 10^{-7} to 10^{-8} meters.[1] The scale of the external electric field is obtained by following the available literature.[2–4] In such case, the external electric field with this magnitude $O\left[10^3\right]$ does not perturb the charge distribution obtained under the influence of the induced electric field, and it does not even perturb the other physical quantities as well.[1,4] The perturbation in ϕ_I represented as $\phi_I = \phi_{I_{eq}} + \delta\phi_I$ can be simplified as $\phi_I \sim \phi_{I_{eq}}$ since $\delta\phi_I \to 0$. Note that $\phi_{I_{eq}}$ is the induced electrostatic potential obtained at the equilibrium.[4] The perturbation $\delta\phi_I$ depends on the ratio of external electric field strength to the induced electric field strength, and particularly in the present study, this ratio tends to zero according to the above discussion. The effect of such external field modulated perturbation is notable when the magnitude of the external electric field is sufficiently high.[1,4] Therefore, in the present study, the weak-field approximation $\left(\nabla\Phi \sim \nabla\phi_I\right)$ holds, and the ionic distribution n_i, according to Eq. (1) depends only on the induced electrostatic potential ϕ_I.

S2. Comparison of the present method with the FEM based COMSOL Multiphysics

In Fig. S1, we compare our results with those obtained from the FEM based solver COMSOL Multiphysics™. While modeling the problem in COMSOL framework, we have used the same set of transport equations and boundary conditions as detailed in section II(E). The chosen mesh counts (22582) in COMSOL solver ensure greater accuracy of the results. In Fig. S1, the results of the present modeling framework show both qualitative and quantitative agreement with the results of COMSOL solver.

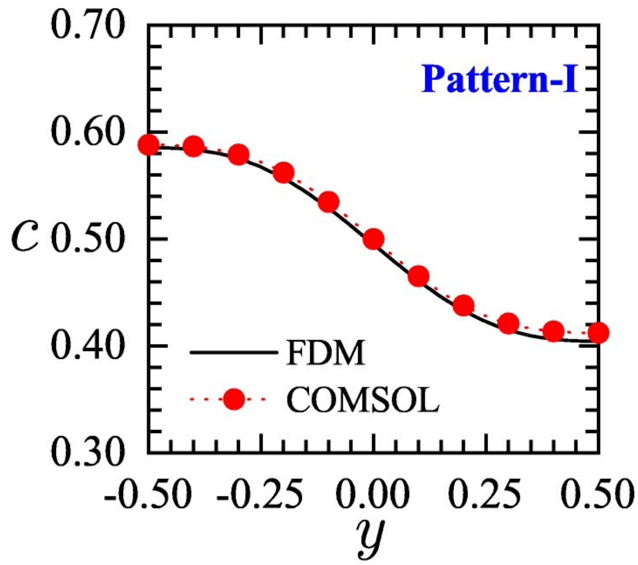

Figure S1 (colour online): Validation with FEM: Plots showing the comparison between the concentration profiles obtained from the FDM and FEM (COMSOL) methods. The profiles are obtained at the outlet of the channel, i.e. at $x = 5$. The other parameters are: $U_{in} = 0.1$, $Re = 0.001$, $Sc = 5 \times 10^5$, $\kappa = 15$, $d = 0.1$, $\alpha = 10$ and $\kappa_p = 10$.

S3. Estimation of Ionic peclet number through the order of magnitude analysis

In the present study, the height of the channel ranges in $O\left[10^{-6} - 10^{-7}\right]$ meters, and according to the weak-field approximation, the external electric field strength has magnitude $O\left[10^{3}\right]$V/m (explained before). For dilute electrolytic solutions, the ionic diffusivity $\left(D_i\right)$ ranges in the limits $O\left[10^{-8} - 10^{-9}\right]$m^2/s.[1,5] With these parameters, the scale of U_{HS} can be estimated as $O\left[10^{-5}\right]$ m/s, and that of ionic Peclet number $\left(\mathrm{Pe_I}\right)$ can be estimated in the range of 10^{-2} to 10^{-4}. This scale of $\mathrm{Pe_I}$ is also analogous to the estimation of Zaccone et al.[6] As a result, the convective effects in ionic transport [Eq. (3)] can be considered as negligible in the present study. Moreover, ionic transport can be assumed to achieve the steady-state phenomenon at the earliest due to dominating diffusion effects $\left(\mathrm{Pe_I} \sim O\left[10^{-2} - 10^{-4}\right]\right)$. Therefore, Eq. (3) can be simplified as:

$$0 = \overline{\nabla}^2 \overline{n}_i + \overline{\nabla}.\left(\overline{n}_i \overline{\nabla} \overline{\phi}_I\right) \tag{S1}$$

Now using the electroneutrality condition ($\overline{n}_i = 1$ at $\overline{\phi}_I = 0$) and the no-flux condition ($\partial \overline{n}_i = 0$ at $\partial \overline{\phi}_I = 0$), we obtain the Boltzmann ion distribution as:

$$\bar{n}_i = \exp\left(-\bar{\phi}_I\right) \tag{S2}$$

S4. Vortex shifting phenomenon: Effect of the PEL thickness d

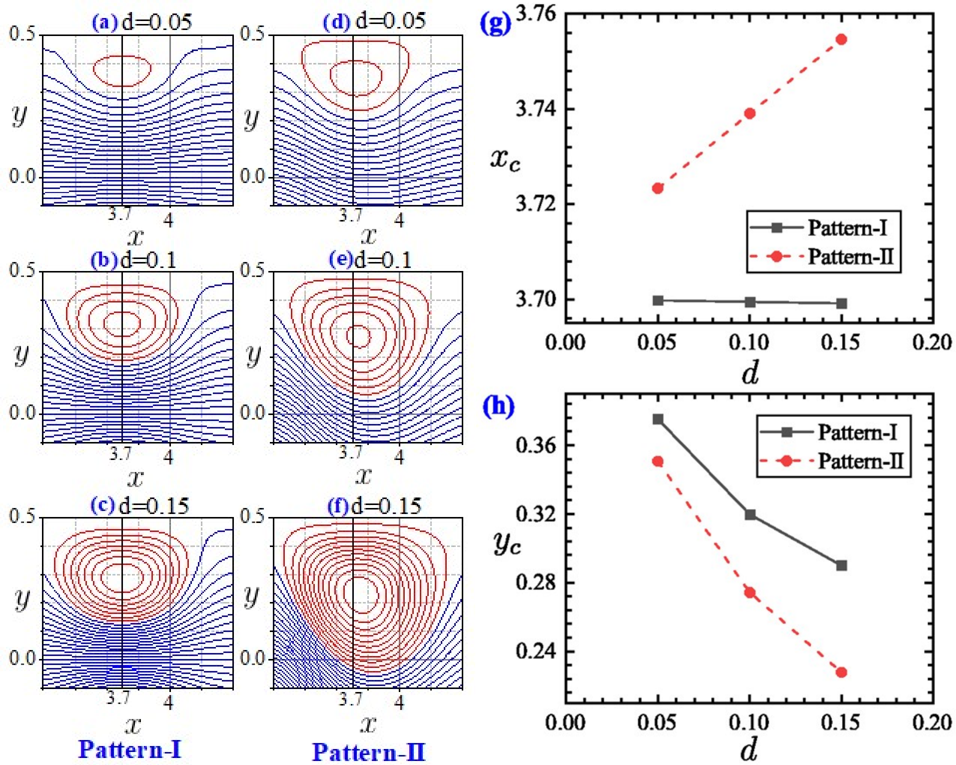

Figure S2 (colour online): **Qualitative analysis of vortex shifting (Panel-A):** Contour plots in Figs. (a)-(c) and Figs. (d)-(f) showing the zoomed-in view of recirculation zones for pattern-I and pattern-II, respectively. The plots are obtained at the upper wall for PEL patch grafted at $x = 3.7$, for different values of PEL thickness $d = 0.05, 0.1, and\ 0.15$. The other parameters are $\kappa = 15$, $\kappa_p = 10$, $\alpha = 10$, $Sc = 5 \times 10^5$, $Re = 10^{-3}$ and $U_{in} = 0.1$. **Quantitative analysis of vortex shifting (Panel-B):** The line plots in Fig. (g) and Fig. (h) showing the variation in the x location and y location of the vortex centroid, respectively. The plots are obtained for both the patterns: pattern-I and pattern-II, with the variation in the PEL thickness d.

In Figs. S2(a)-(h), we make an effort to quantify the vortex dynamics as realizable through the loci of their centroids. We observe in Figs. S2(a)-(h) that, for the higher value of PEL thickness $d = 0.15$, the vertical shift in the centroid of the vortex is high for pattern-II. We have discussed that the PEL thickness is a contributing factor for the strength and the size of the recirculation zones being formed. Accounting this fact, for the patterns considered here, the size and height of the vortices is expected to increase with an increment in PEL thickness d. (Height of the vortex refers to the distance of its centroid from the nearest wall). However, for the case of pattern-I, the vortices shed on the lower wall approach to those of the upper wall in *face-to-face* mode as they are symmetric about the channel centerline. Notably, this *face-to-face* approaching kinetics of vortices limits the shifting of the centroid (both lateral and vertical) with a variation in PEL thickness, d as seen in Figs. 5(aa)-(dd), S2(a)-(c) and S2(h). Whereas in pattern-II configuration, the asymmetric formation of vortices prohibits them from approaching via the *face-to-face* mode (vortices form at the lower wall: $x = 3.1$ and at the upper wall: $x = 3.7$).

As such, this unobstructed dynamics of the vortices for pattern-II configuration allow them to expand towards the central region of the channel (see Figs. S2(d)-(f)). Therefore, for pattern-II configuration, we observe a significant vertical shift in the centroid of the vortices with an increment in PEL thickness d, as witnessed in Figs. S2(d)-(f). Further, this asymmetric flow structure in pattern-II configuration creates the distorted streamlines in the flow field, presented in Figs. 5(cc)-(dd). Consequently, for pattern-II, the diverted flow field around any vortex disturbs the formation of the vortex at the next consecutive position, causing a lateral stretching in particular (cf. Fig. S2(g)). Moreover, with an increment in PEL thickness d, this lateral displacement intensifies (see Fig. S2(g)), primarily attributed to the enhancement of electroosmotic flow strength.

References

1 J. H. Masliyah and S. Bhattacharjee, *Electrokinetic and Colloid Transport Phenomena*, Wiley, 2006.

2 P. K. Mondal, U. Ghosh, A. Bandopadhyay, D. DasGupta and S. Chakraborty, *Soft Matter*, 2014, **10**, 8512–8523.

3 R. Peng and D. Li, *Nanoscale*, 2016, **8**, 12237–12246.

4 D. A. Saville, *Annu. Rev. Fluid Mech.*, 1977, **9**, 321–337.

5 R. J. Hunter, *Zeta Potential in Colloid Science: Principles and Applications*, Academic Press, London, 1981.

6 A. Zaccone, H. Wu, D. Gentili and M. Morbidelli, *Phys. Rev. E*, 2009, **80**, 1–8.